| RESEARCH ARTICLE | OPEN ACCESS |

Subthalamic Deep Brain Stimulation: Mapping Non-Motor Outcomes to Structural Connections

Garance M. Meyer[1] 📷 | Ilkem Aysu Sahin[2,3,4] | Barbara Hollunder[2,3,4] 📷 | Konstantin Butenko[1] | Nanditha Rajamani[1,2,3,4] | Clemens Neudorfer[1,5] | Lauren A. Hart[1] | Jan Niklas Petry-Schmelzer[6] | Haidar S. Dafsari[6] 📷 | Michael T. Barbe[6] | Veerle Visser-Vandewalle[7] | Philip E. Mosley[8,9,10,11] 📷 | Andreas Horn[1,2,3,5]

[1]Center for Brain Circuit Therapeutics, Department of Neurology, Brigham & Women's Hospital, Harvard Medical School, Boston, Massachusetts, USA | [2]Movement Disorders and Neuromodulation Unit, Department of Neurology, Charité – Universitätsmedizin Berlin, Berlin, Germany | [3]Einstein Center for Neurosciences Berlin, Charité – Universitätsmedizin Berlin, Berlin, Germany | [4]Berlin School of Mind and Brain, Humboldt-Universität Zu Berlin, Berlin, Germany | [5]Department of Neurosurgery, Massachusetts General Hospital, Harvard Medical School, Boston, Massachusetts, USA | [6]Department of Neurology, Faculty of Medicine and University Hospital, University of Cologne, Cologne, Germany | [7]Department of Stereotactic and Functional Neurosurgery, Faculty of Medicine and University Hospital, University of Cologne, Cologne, Germany | [8]Clinical Brain Networks Group, QIMR Berghofer Medical Research Institute, Brisbane, Queensland, Australia | [9]Neurosciences Queensland, St Andrew's War Memorial Hospital, Brisbane, Queensland, Australia | [10]Queensland Brain Institute, University of Queensland, Brisbane, Queensland, Australia | [11]Australian eHealth Research Centre, CSIRO Health and Biosecurity, Brisbane, Queensland, Australia

Correspondence: Garance M. Meyer (gmeyer3@bwh.harvard.edu)

ABSTRACT

In Parkinson's Disease (PD), deep brain stimulation of the subthalamic nucleus (STN-DBS) reliably improves motor symptoms, and the circuits mediating these effects have largely been identified. However, non-motor outcomes are more variable, and it remains unclear which specific brain circuits need to be modulated or avoided to improve them. Since numerous non-motor symptoms potentially respond to DBS, it is challenging to independently identify the circuits mediating each one of them. Data compression algorithms such as principal component analysis (PCA) may provide a powerful alternative. This study aimed at providing a proof of concept for this approach by mapping changes along extensive score batteries to a few anatomical fiber bundles and, in turn, estimating changes in individual scores based on stimulation of these tracts. Retrospective data from 56 patients with PD and bilateral STN-DBS was included. The patients had undergone comprehensive clinical assessments covering changes in appetitive behaviors, mood, anxiety, impulsivity, cognition, and empathy. PCA was implemented to identify the main dimensions of neuropsychiatric and neuropsychological outcomes. Using DBS fiber filtering, we identified the structural connections whose stimulation was associated with change along these dimensions. Then, estimates of individual symptom outcomes were derived based on the stimulation of these connections by inverting the PCA. Finally, changes along a specific non-motor score were estimated in an independent validation dataset ($N = 68$) using the tract model. Four principal components were retained, which could be interpreted to reflect (i) general non-motor improvement; (ii) improvement of mood and cognition and worsening of trait impulsivity; (iii) improvement of cognition; and (iv) improvement of empathy and worsening of impulsive-compulsive

behaviors. Each component was associated with the stimulation of spatially segregated fiber bundles connecting regions of the frontal cortex with the subthalamic nucleus. The extent of stimulation of these tracts was able to explain significant amounts of variance in outcomes for individual symptoms in the original cohort (circular analysis), as well as in the rank of depression outcomes in the independent validation cohort. Our approach represents an innovative concept for mapping changes along extensive score batteries to a few anatomical fiber bundles and could pave the way toward personalized deep brain stimulation.

1 | Introduction

Deep brain stimulation (DBS) is used as a treatment for a range of neurological and psychiatric disorders, such as Parkinson's disease (PD), essential tremor, obsessive-compulsive disorder, or major depressive disorder (Lozano et al. 2019). Delivering stimulation to the correct target is key to treatment efficacy. DBS network mapping and DBS fiber filtering have emerged as promising techniques to identify specific brain networks or connections whose modulation may contribute to DBS outcomes (Horn and Fox 2020; Middlebrooks et al. 2020). These methods demonstrated the ability to estimate outcomes in independent cohorts (Gadot et al. 2024; Horn et al. 2017; Irmen et al. 2020; Li et al. 2020; Smith et al. 2021) and prospective patients (Hollunder et al. 2024; Rajamani et al. 2024). Hence, this work may inform DBS programming in future patients through the use of algorithms aimed at maximally engaging networks associated with therapeutic effects while avoiding engagement of networks associated with side effects (Hollunder et al. 2022).

Still, previous studies typically analyzed stimulation impact on a single clinical score, such as UPDRS-III in PD or Y-BOCS in obsessive-compulsive disorder, which resulted in a single target circuit (Horn et al. 2017, 2019; Li et al. 2020; Neudorfer et al. 2023). In contrast, many of the disorders treated with DBS are complex and multi-symptomatic. In this light, a strategy relying on repeated independent application of the method for each single score would rapidly become prone to alpha error accumulation. Moreover, in some cases, different symptoms may map to partially shared neural substrates (Cuthbert and Insel 2013; Insel et al. 2010), rendering this approach conceptually suboptimal, too.

Non-motor outcomes of subthalamic nucleus (STN) DBS in Parkinson's disease represent a good example of this issue, since numerous neuropsychological and neuropsychiatric symptoms may be of interest (Mosley et al. 2018; Petry-Schmelzer et al. 2019). While often overlooked, non-motor symptoms bear a large contribution to the quality of life in patients with PD (Antonini et al. 2012; Barone et al. 2009; Floden et al. 2014; Martinez-Martin 2011). Indeed, it was shown that the total burden of non-motor symptoms on quality of life surpasses that of motor symptoms (Martinez-Martin 2011; Martinez-Martin et al. 2009). While motor symptoms and complications are improved by DBS in most patients (Deuschl et al. 2006; Kleiner-Fisman et al. 2006; Schuepbach et al. 2013; Weaver et al. 2009), non-motor outcomes are variable (Dafsari et al. 2016; Fasano et al. 2012; Volkmann et al. 2010; Voon et al. 2006). For example, increased apathy is a common concern in patients receiving STN-DBS, whereas some patients demonstrate improvement in apathy instead (Béreau et al. 2023; Thobois et al. 2010). Impulsive-compulsive behaviors often improve after STN-DBS but have also been reported to develop de novo in some patients (Abbes et al. 2018; Kim et al. 2018;

Lhommée et al. 2018). Similar variability in outcomes is observed for other symptoms such as cognitive decline, depression, or anxiety (Castelli et al. 2006; Mosley et al. 2018; Reich et al. 2022). This variability in outcomes likely depends at least in part on factors such as patient characteristics and dopaminergic treatment management, but stimulation itself and choice of parameters also play a role (Bejjani et al. 1999; Béreau et al. 2023; Castrioto et al. 2014; Mosley et al. 2018; Mosley, Paliwal, et al. 2020; Petry-Schmelzer et al. 2019; Prange et al. 2022; Welter et al. 2014; Witt et al. 2013), consistent with the known involvement of the STN in associative and limbic cortico-basal ganglia loops (Emmi et al. 2020; Haynes and Haber 2013). Still, the circuits contributing to neuropsychiatric and neuropsychological outcomes are far less established than those contributing to motor outcomes. Since changes in these symptoms are delayed and cannot be immediately and objectively quantified when stimulation parameters are adjusted, identifying reliable and objective relationships between stimulated circuits and the changes in these symptoms may help DBS programming significantly.

Here, we propose a novel approach that aims at (i) condensing a larger battery of scores onto a few main dimensions, (ii) identifying the structural connections associated with each dimension, and (iii) estimating changes in individual scores based on stimulation of the identified tracts. Conceptually, the approach is powerful since it projects a high-dimensional score battery onto a low-dimensional architecture of tracts, only to expand results to estimate changes within the high-dimensional score battery again. We use the example of non-motor symptoms in PD as a use case to explore the approach, applying it to a cohort of 56 patients with PD and STN-DBS, in which non-motor outcomes have been comprehensively recorded. We must emphasize that the focus of this study was methodological rather than clinical. In other words, the main purpose of the present study was to provide a proof-of-concept for the proposed approach, rather than to produce a reliable and clinically meaningful model. Still, we used a second cohort of 68 patients with PD to validate a subset of our results.

2 | Methods

2.1 | Patients and Assessments

The main cohort consisted of 60 patients with PD who were recruited and received bilateral STN-DBS at the Asia-Pacific Centre for Neuromodulation in Brisbane, Australia. Inclusion criteria were: diagnosis of PD according to the UK Brain Bank criteria (Hughes et al. 1992), Hoehn and Yahr stage 2 or greater with motor fluctuations or other motor complications related to dopaminergic therapy, and absence of dementia at baseline as defined following the Movement Disorder Society criteria (Emre et al. 2007). Detailed clinical procedures have been

TABLE 1 | Patient characteristics for the main cohort.

	Preoperative	Postoperative	Pre. vs. Post. [range]
Characteristics			
N patients	*N* = 56		—
Sex	19 F/37 M		—
Age at surgery	62.2 ± 9.4		—
Disease duration	8.0 ± 4.0		—
Follow-up time	6 months		—
Electrode model	Abbott 6172, *N* = 17 Medtronic 3389, *N* = 23 B. Sci. Vercise Standard, *N* = 16		—
LEDD (mg)	1126 ± 633	360 ± 250	*p* < 0.001* [−300; 3150]
UPDRS-III, on medication	39.0 ± 14.6	36.2 ± 13.5	*p* = 0.19 [−34; 39]
Neuropsychological assessments			
SAS	12.0 ± 4.8	12.5 ± 6.3	*p* = 0.49 [−14; 9]
BDI	11.0 ± 5.3	9.0 ± 6.4	*p* = 0.008* [−15; 12]
GAI	5.1 ± 4.5	3.9 ± 5.5	*p* = 0.01* [−8; 10]
QUIP-RS	20.3 ± 15.7	18.0 ± 14.4	*p* = 0.28 [−39; 46]
BIS-11 att.	15.1 ± 2.8	15.2 ± 3.2	*p* = 081 [−6; 7]
BIS-11 mot.	20.9 ± 3.0	21.1 ± 2.9	*p* = 0.63 [−7.5; 7]
BIS-11 non-p.	22.2 ± 4.1	23.3 ± 4.6	*p* = 0.01* [−9; 6.5]
EQ	39.1 ± 11.2	38.5 ± 12.7	*p* = 0.52 [−13.5; 13.5]
MoCA	25.9 ± 2.3	26.0 ± 2.9	*p* = 0.68 [−4; 6]
MMSE	28.2 ± 1.5	28.3 ± 1.9	*p* = 0.55 [−3; 4]

Note: p-values are given for a paired sample *t*-test (df = 55, two-tailed), not corrected for multiple comparisons. * indicates statistical significance at *p* < 0.05. The range of absolute changes is given such as positive values representing improvements, while negative values represent worsening (see text for details). Note that BIS and EQ scores were averaged between patient self-ratings and caregiver ratings.

Abbreviations: BDI, Beck Depression Inventory; BIS, Barratt Impulsiveness Scale; EQ, Empathy Quotient; GAI, Geriatric Anxiety Inventory; LEDD, Levodopa equivalent daily dose; MMSE, mini-mental state evaluation; MoCA, Montreal cognitive assessment; QUIP-RS, questionnaire for impulsive and compulsive behaviors rating scale; SAS, Starkstein apathy scale; UPDRS-III, unified Parkinson's disease rating scale part III.

reported in previous publications (Mosley, Paliwal, et al. 2019, 2020; Mosley, Robinson, et al. 2020). Patients were assessed preoperatively and 6 months postoperatively (ON stimulation) while receiving their usual dopaminergic medication. The assessments comprised the Unified Parkinson's Disease Rating Scale—Part III (UPDRS-III) as well as an extensive neuropsychiatric and neuropsychological battery including the Starkstein Apathy Scale (SAS) (Starkstein et al. 1992), the Beck Depression Inventory (BDI) (Beck et al. 1961), the Geriatric Anxiety Inventory (GAI) (Pachana et al. 2007), the Questionnaire for Impulsive and Compulsive Behaviors Rating Scale (QUIP-RS) (Weintraub et al. 2012), the Barratt Impulsiveness Scale (BIS-11) (Patton et al. 1995), the Empathy Quotient (EQ) (Baron-Cohen and Wheelwright 2004), the Montreal Cognitive Assessment (MoCA) (Nasreddine et al. 2005), and the Mini-Mental State Evaluation (MMSE) (Folstein et al. 1975). In addition to these questionnaires and rating scales, the battery included three behavioral assessments, namely, the Hayling Sentence Completion Test (Burgess and Shallice 1997), the Excluded Letter Fluency Test (Shores et al. 2006), and the Delay Discounting Task (Kirby

et al. 1999), and the Levodopa equivalent daily dose (LEDD) was recorded. The BIS-11 and EQ were filled both by the patients and their caregivers, and these scores were averaged, except for four patients with missing caregiver ratings. There were no other missing values in the neuropsychological assessments.

Different electrode models were implanted, including directional (Abbott 6172, *N* = 17) and non-directional electrodes (Medtronic 3389, *N* = 23; Boston Vercise Standard, *N* = 16). Preoperative (T1- and T2-weighted MRI) and postoperative imaging (CT) were performed to verify accurate electrode placement. For the present study, four patients were excluded from further analyses, owing to missing data (*N* = 1) or inability to reconstruct electrode orientation (*N* = 3; see below). This led to a final sample of 56 patients (Table 1).

An independent cohort of 70 PD patients with bilateral STN-DBS and preoperative and postoperative BDI assessment was used as a validation dataset (Charité Universitätsmedizin Berlin, *N* = 32, and Cologne University Hospital, *N* = 38; Irmen et al. 2020). Two

TABLE 2 | Patient characteristics for the validation cohort.

	Berlin	**Cologne**	**Total**	**Vs. main cohort**
N patients	*N* = 32	*N* = 36	*N* = 68	
Sex	10 F/22 M	18 F/18 M	28 F/40 M	$\chi^2 = 0.7$, $p = 0.41$
Age at surgery	61.4 ± 9.8	62.0 ± 8.2	61.7 ± 9.0	$p = 0.80$
Disease duration	10.3 ± 4.9	10.4 ± 3.9	10.4 ± 4.4	$p = 0.002$
Follow-up time	12 months	6 months		
Electrode model	Medtronic 3389, *N* = 18 Boston Sci. Vercise Standard, *N* = 7 Boston Sci. Vercise Directed, *N* = 7	Medtronic 3389, *N* = 1 Boston Sci. Vercise Standard, *N* = 4 Boston Sci. Vercise Directed, *N* = 31		
LEDD (mg)				
Preoperative	1185 ± 685	1121 ± 450	1151 ± 569	$p = 0.82$
Postoperative	559 ± 344*	552 ± 244*	555 ± 293*	$p < 0.001$
UPDRS-III, on med.				
Preoperative	20.8 ± 10.3	17.8 ± 9.9	19.1 ± 10.1	$p < 0.001$
Postoperative	19.3 ± 13.8	17.1 ± 8.9	18.1 ± 11.5	$p < 0.001$
BDI				
Preoperative	11.6 ± 6.3	7.0 ± 4.3	9.1 ± 5.7	$p = 0.06$
Postoperative	11.6 ± 7.5	7.3 ± 5.8	9.3 ± 6.9	$p = 0.79$

Note: p-values are given for a two-sample *t*-test comparing characteristics of the validation and main cohorts, unless stated otherwise.
Abbreviations: BDI, Beck depression inventory; LEDD, Levodopa equivalent daily dose; UPDRS-III, unified Parkinson's disease rating scale part III.
*Indicate a statistically significant difference between preoperative and postoperative scores in the validation cohort (paired *t*-tests).

patients from the Cologne cohort were excluded from the analyses based on significant psychiatric comorbidities at the time of BDI assessment, leading to a final validation sample of 68 patients (Table 2).

Written informed consent was obtained from all patients at the time of recruitment. Secondary data analysis for the present study was approved by the Institutional Review Board of the Brigham and Women's Hospital in agreement with the Declaration of Helsinki.

2.2 | Principal Component Analysis

PCA was performed to identify the principal dimensions of non-motor outcomes in the main cohort. We focused on change in neuropsychiatric symptoms as assessed by rating scales and questionnaires (*N* = 10 variables, i.e., the SAS, BDI, GAI, QUIP-RS, BIS-11 attentional, motor and non-planning sub-scores, EQ, MoCA, and MMSE). In other words, the behavioral assessments (i.e., the Hayling Test, Excluded Letter Fluency Test, and Delay Discounting Task) were not included in the PCA. The reasons for this choice are twofold: first, this avoided obtaining a principal component that would simply oppose assessments of a different nature (behavioral vs. questionnaires and rating scales; see e.g., Reynolds et al. 2006). Second, the behavioral assessments correlated poorly not only with the questionnaires but also with each other, meaning

that they were less amenable to dimensionality reduction. Moreover, the BIS-11 sub-scores were used instead of the total score since changes along these sub-scores did not strongly correlate with each other and since there was sufficient variance along each of the sub-scores.

PCA was calculated on absolute change scores along the 10 retained variables. To facilitate the interpretation of the principal components (PCs), all change scores were computed such that positive values would denote improvement of symptoms, and negative values would denote worsening. In other words, changes in MMSE, MoCA, and EQ, for which higher scores respectively represent better cognition or empathy, were computed as (postoperative—preoperative score). The data was z-scored before computing the PCA, which was done using the "pca" Matlab function (Matlab R2022b).

The number of PCs to retain was determined based on the standard criterion of eigenvalue > 1, the cumulative explained variance, and the interpretability of the PCs, leading to the retention of four PCs (see Section 3).

2.3 | Electrode Localizations and Electric Field Modeling

The Lead-DBS toolbox (v3; www.lead-dbs.org; Neudorfer et al. 2023) was used to localize the DBS electrodes and model

the electric fields (E-fields). The standard analysis pipeline was used (Horn et al. 2019; Horn and Kühn 2015; Neudorfer et al. 2023). First, the available preoperative and postoperative images were co-registered using SPM12 for MRI scans (Friston et al. 2007) and ANTs for CT scans (Avants et al. 2011). Then, the images were normalized to template "MNI" space (ICBM 2009b Nonlinear Asymmetric) using the ANTs-SyN algorithm (Avants et al. 2011) with the default presets implemented in Lead-DBS (Ewert et al. 2019). Non-linear brain shift correction was applied to the postoperative CT scans to account for potential pneumocephalus (Horn and Kühn 2015). Finally, electrode trajectories were reconstructed using the PaCER algorithm (Husch et al. 2018), and where applicable, electrode orientation was detected using the DiODe algorithm (Dembek et al. 2021). The image quality and results of each step were carefully verified by visual inspection. Manual refinements of normalization and electrode reconstruction were performed as needed using dedicated tools (Neudorfer et al. 2023; Oxenford et al. 2024).

E-field modeling was performed to estimate the extent of the stimulated tissue depending on the clinical stimulation parameters (i.e., active contacts and amplitude). For this purpose, the OSS-DBS model was applied, as implemented in Lead-DBS (Butenko et al. 2020; Neudorfer et al. 2023). Briefly, OSS-DBS employs a finite element model to estimate the E-field in a 3D domain represented by a curved mesh with discrete conductivity values defined for cerebrospinal fluid, white matter, and grey matter. The estimation was performed in the native patient space, and the resulting E-field magnitude maps were warped into MNI space using the previously computed transformation matrices.

2.4 | Structural Connectivity Analysis

2.4.1 | Development of the Four-Tract Model

We used the DBS fiber filtering approach (Baldermann et al. 2019; Li et al. 2020; Neudorfer et al. 2023), which relies on normative brain connectomes, to identify fiber tracts whose stimulation was associated with DBS effects. While this method has often been used to identify fiber tracts associated with optimal clinical outcomes (Baldermann et al. 2019; Horn et al. 2022; Li et al. 2020; Ríos et al. 2022), here, we adapted the method to identify fiber tracts associated with high or low PC scores, i.e., with variance along the identified principal dimensions of non-motor outcome (see Figure 1 for schematic depiction of the method). The entire analysis pipeline was implemented and is openly available within the Lead-DBS "fiber filtering explorer" (https://github.com/netstim/leaddbs) (Neudorfer et al. 2023).

An extended version of the DBS tractography atlas (Middlebrooks et al. 2020) was used as a connectome. This connectome was created using DSI studio (Yeh et al. 2013), based on a diffusion template derived from the data of 1065 healthy participants from the Human Connectome Project (Van Essen et al. 2012; Yeh 2022) and with a particular focus on STN connections. The resulting tracts have been compared to macroscopic and microscopic data as well as tracing studies and anatomically validated

by neuroanatomy and neuro-imaging experts. A complete description of these procedures has been published elsewhere (Rajamani et al. 2024).

Each fiber of the connectome was assigned four values, each representing the association between stimulation of this fiber and scores for one of the four PCs across the patient cohort. Specifically, these values consisted of Pearson correlation coefficients—calculated across patients—between the probabilistic impact of each E-field on the fiber (i.e., peak E-field value along the fiber) and the corresponding PC scores. In other words, for each PC, positive R-values were attributed to fibers preferentially stimulated in patients who scored high on this given PC, while negative *R*-values were attributed to fibers preferentially stimulated in patients who scored low on this given PC. Similar to previous studies (Hollunder et al. 2024; Li et al. 2020; Rajamani et al. 2024), the goal of this procedure was not to assess which individual fibers are significantly associated with PC scores, which would require testing for statistical significance of the *R* values with appropriate correction for multiple comparisons. Rather, this procedure aimed to identify and visualize the fiber tracts demonstrating the strongest positive or negative associations with PC scores. For each PC, the top 1000 fibers with the strongest positive and top 1000 fibers with the strongest negative *R*-values were retained as part of the tract model. Importantly, "impact" of E-fields on each fiber is inherently the same across PCs, such that any segregation of tracts across PCs is a result of differential association of stimulated fibers with PC scores.

Of note, only fibers traversing at least 20% of the E-fields with peak E-field magnitudes above 200 V/m (corresponding to the standard threshold used for the computation of so-called "volumes of tissue activated"; Åström et al. 2015) were considered for analysis. The rationale was to exclude fibers that were not affected by strong E-fields in at least a fraction of cases, or in other words, not modulated (above threshold) for many patients.

Furthermore, given the known association of non-motor symptoms such as apathy, depression, and impulsive-compulsive behaviors with dopaminergic medication or state (Czernecki et al. 2008; Thobois et al. 2010; Weintraub et al. 2010), we controlled for the reduction in dopaminergic treatment by using partial correlation between peak E-field values and PC scores accounting for LEDD change rather than simple correlation.

2.4.2 | Estimates of Outcomes

To obtain estimates of outcomes for the 10 clinical assessments based on our four-tract model, we first derived estimates of PC scores based on the overlap of the E-field with the retained positive and negative tracts, and then used the PCA weights to map these estimates back to the original variables.

Specifically, for each patient and PC, estimates of PC scores were obtained by computing the weighted sum of R values corresponding to the fibers traversing the patient's E-fields. For example, a patient whose E-fields would peak at sites corresponding to tracts positively associated with PC2 but located in close
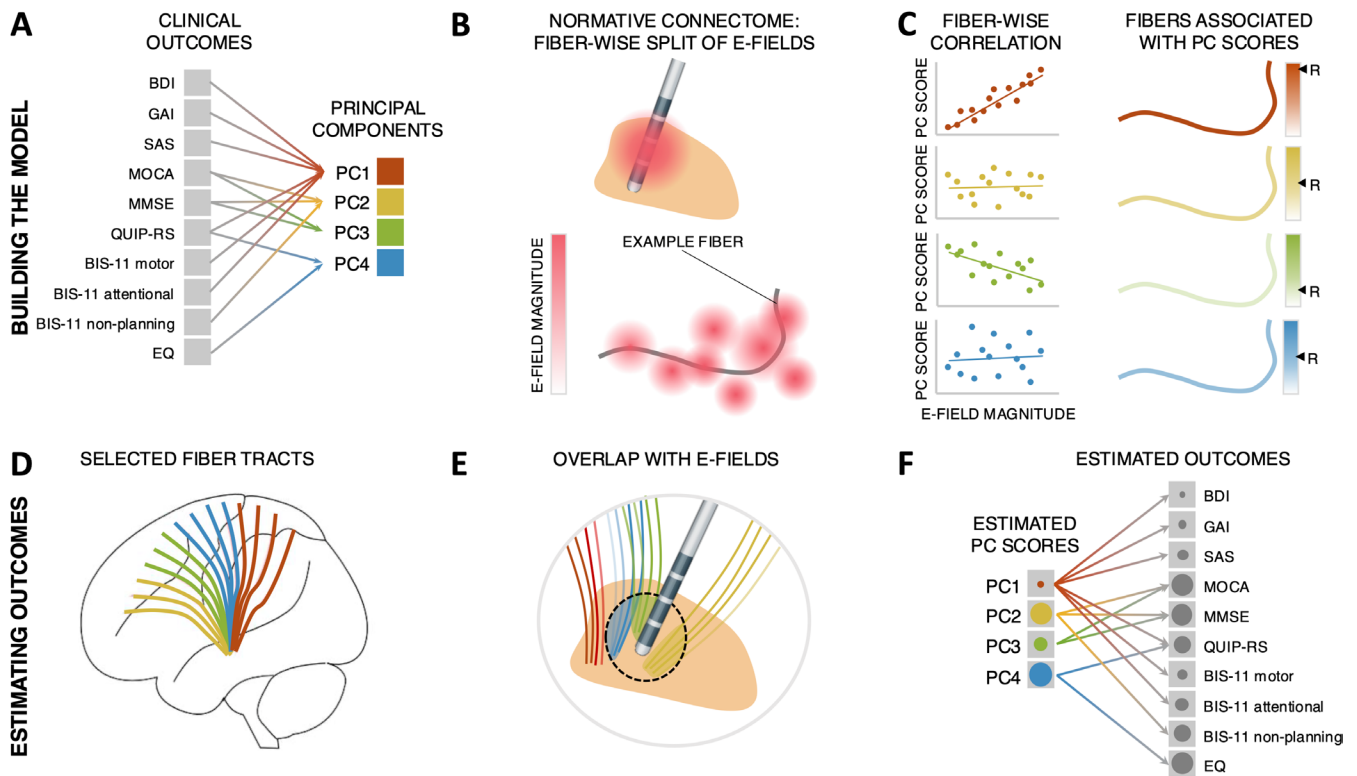
FIGURE 1 | Development of the four-tract model. (A) Principal component analysis (PCA) was performed to identify the principal dimensions of non-motor outcomes. Then, the fiber tracts whose stimulation was associated with variance along these four dimensions were identified using DBS fiber filtering. (B) For each fiber in a normative pathway atlas, the probabilistic impact of each E-field on the fiber was estimated by taking the peak E-field value along the fiber. (C) These values were then correlated with PC scores. Hence, for each PC, positive R-values were attributed to fibers preferentially stimulated in patients who scored high on this given PC, while negative *R*-values were attributed to fibers preferentially stimulated in patients who scored low on this given PC. (D) The top 1000 positive and negative fibers (strongest positive and negative *R*-values) were retained as part of the four-tract model. (E) Overlap between E-fields and these fibers was used to obtain estimates of PC scores, which were then mapped back to estimates for the original variables by applying PCA weights (F). BDI, Beck depression inventory; BIS-11, Barratt impulsiveness scale; EQ, empathy quotient; GAI, geriatric anxiety inventory; MMSE, mini-mental state examination; MoCA, Montreal cognitive assessment; QUIP-RS, questionnaire for impulsive and compulsive behaviors rating scale; SAS, Starkstein apathy scale.

vicinity to tracts negatively associated with PC3 would receive a high estimate for PC2 and a low estimate for PC3. Finally, matrix multiplication of these estimates by PCA weights allowed us to recover estimates for each of the 10 clinical assessments. Correlation coefficients between estimated and observed outcomes were calculated to estimate the accuracy of the model. However, since estimates are derived in a circular fashion (i.e., the tract model was calculated on the same data points as those used to test it), and despite the fact that most of those would fall below the standard threshold for statistical significance ($R = 0.38$–0.66, see Section 3), we refrain from reporting associated *p*-values. Cross-validation was performed using different designs (5-fold, 10-fold, leave-one-out) as previously described (e.g., Rajamani et al. 2024).

2.5 | Out-of-Sample Validation

In order to evaluate the robustness and generalizability of the model, estimates of BDI outcomes were obtained for the validation cohort based on E-field overlap with the four-tract model as detailed above and subsequently rank-correlated with empirical outcomes. Only estimates for BDI could be tested since only this

score was available for the combined validation cohort (Irmen et al. 2020).

3 | Results

3.1 | Clinical Outcomes and Electrode Positions

The final sample used to build the tract model (main cohort) consisted of 56 PD patients receiving bilateral STN-DBS (19 females, 37 males; age at surgery: 62.2 ± 9.4 years). Patient characteristics are reported in Table 1.

Detailed neuropsychological outcomes have been reported elsewhere (Mosley, Paliwal, et al. 2020; Mosley, Robinson, et al. 2020). Briefly, at the group level, statistically significant pre- to postoperative changes were only seen for depression (BDI; improved, $p = 0.008$), anxiety (GAI; improved, $p = 0.01$), and non-planning impulsivity (BIS-11 non-planning sub-score; worsened, $p = 0.01$; uncorrected *p*-values). However, important variability in outcomes was observed. For example, despite statistically significant improvement in BDI at the group level, changes along this score ranged from a worsening of 15 points
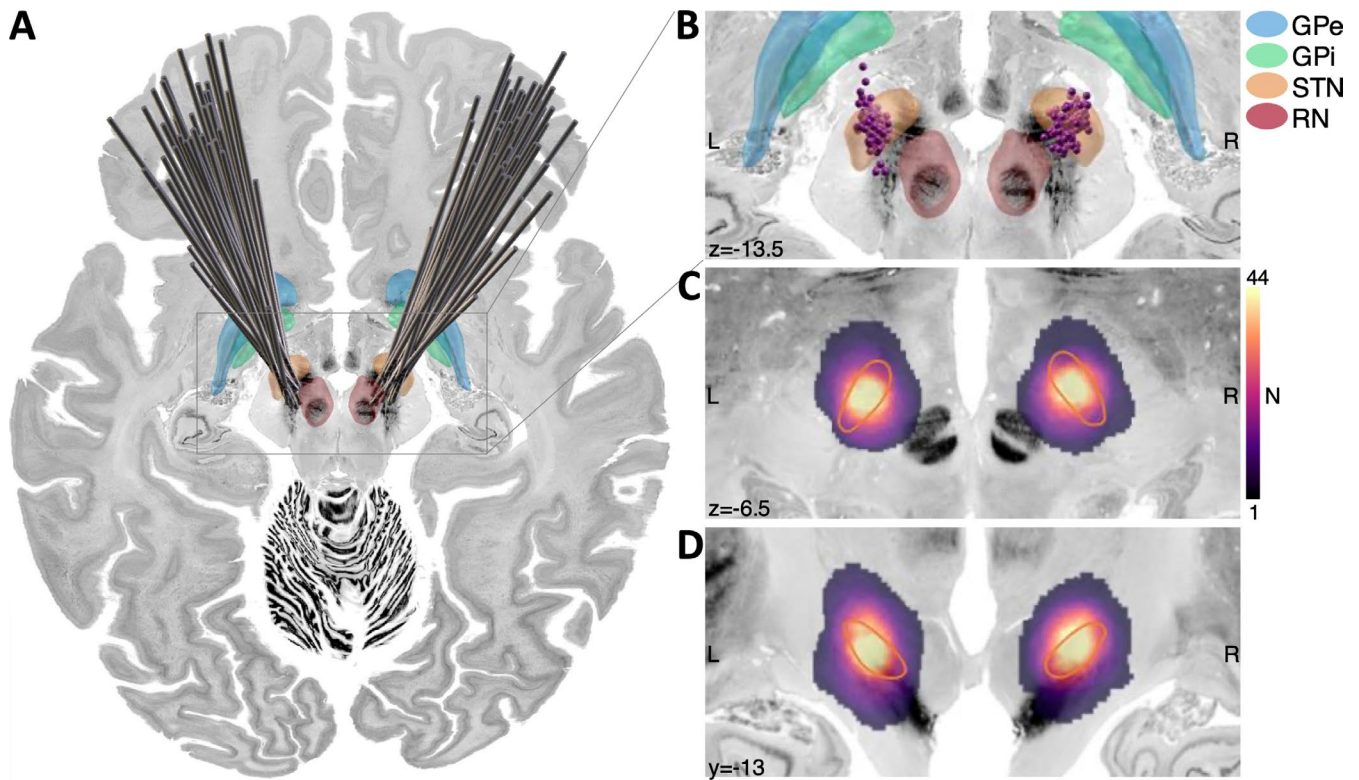
FIGURE 2 | Electrode and active contact locations for the main cohort ($N = 56$). Electrode (A) and active contact locations (B) are shown relative to basal ganglia structures (derived from the DISTAL atlas, Ewert et al. 2018), overlaid on the Big Brain template (Amunts et al. 2013; Xiao et al. 2019; superior view). (C, D) Axial and coronal views of the N-map, representing the number of stimulation volumes (i.e., E-fields thresholded above 200 V/m, Åström et al. 2015) covering each voxel. Greater overlap between the stimulation volumes was seen in the dorsolateral motor region of the STN. GPe, external pallidum; GPi, internal pallidum; RN, red nucleus; STN, subthalamic nucleus.

to an improvement of 12 points in individual patients (average improvement: 2.0 ± 5.5 points; see Table 1 for other scores). This emphasizes the potential relevance of the present approach, which aims at relating part of this observed variance in outcomes to the modulation of specific fiber tracts.

Statistically significant correlations with change in LEDD were found for change in apathy (SAS; $R = 0.27$, $p = 0.03$) and attentional impulsivity (BIS-11 attentional sub-score; $R = 0.26$, $p = 0.05$; all remaining ps > 0.2; uncorrected p-values).

Electrode and active contact positions, as well as the spatial distribution of the thresholded and binarized E-fields (stimulation volumes, or so-called "volumes of tissue activated", Åström et al. 2015) are shown in Figure 2.

3.2 | Principal Component Analysis

Detailed PCA results are available as Tables S1–S4 and Figure S1. Four PCs were retained, which corresponded to a total of 67% of the variance explained. We did not retain additional components since these had eigenvalues < 1 and were less readily interpretable. Further, PC 5 only explained 8.6% of the variance. As a result of this methodological choice, it is mathematically impossible for the tract model to capture more than 67% of the overall variance in clinical outcomes, even under the implausible assumption of a perfect tract model (i.e., a model that would capture 100% of the variance in PC scores).

Typically, PCs should be understood as opposing or grouping variables, whereas the sign of the loadings is arbitrary. However, here, the sign of the loadings must be considered when interpreting how positive and negative fiber tracts relate to improvement along a given clinical score. Hence, to facilitate the interpretation of the tracts, we hereafter refer to PCs as reflecting improvement or worsening of symptoms.

Based on an examination of the loadings and variable contributions, PC1 may be interpreted as reflecting global non-motor outcome, with most variables loading positively onto it (Figure 3A). Of note, unfortunately, a proper UPDRS-III assessment in off-medication states was not available for this cohort, so it could not be directly related to (or included in) the PCA analysis. Still, there was a statistically significant correlation between PC1 scores and LEDD reduction ($R = 0.26$, $p = 0.04$). As mentioned above, despite the sign of PC loadings being arbitrary and not directly interpretable, we hereafter refer to PC1 as reflecting general non-motor improvement. This aims to help the understanding of connectivity results, making it clear that positive tracts for PC1 were associated with higher improvement along the corresponding variables, while negative tracts were associated with lower improvement or worsening along these variables. PC2 opposed improvements in mood, anxiety, apathy, and cognition to improvements in trait impulsivity. Hence, following the same rationale, we refer to this PC as representing improvements in mood and cognition and worsening of trait impulsivity. PC3 mainly represented changes (hereafter referred to as improvement) in cognition. Finally, PC4 opposed improvements
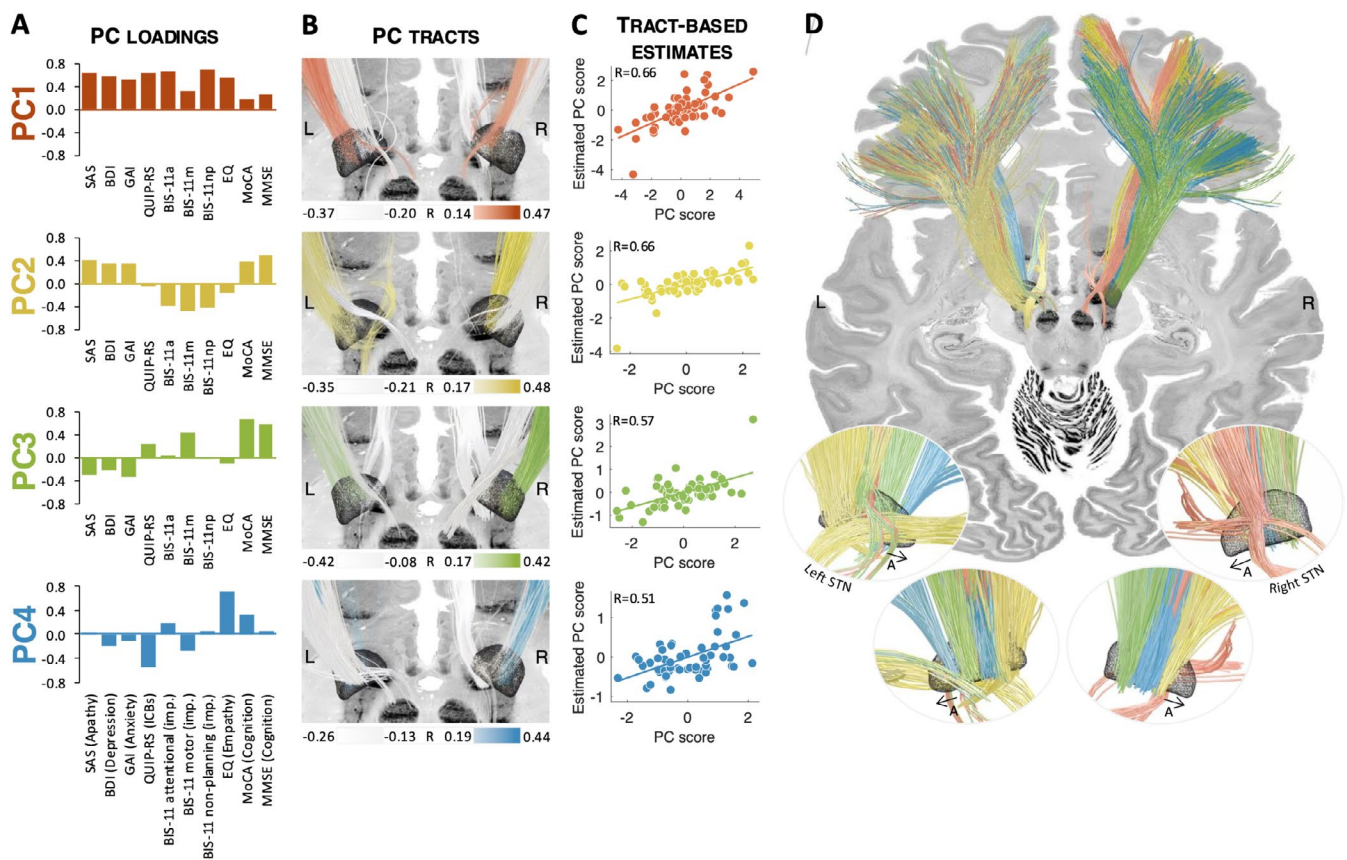
FIGURE 3 | Structural connectivity results. (A) Four principal components were retained which could be interpreted as reflecting general non-motor improvement (PC1), improvement in mood and cognition and worsening in trait impulsivity (PC2), improvement in cognition (PC3), and improvement of empathy and worsening in impulsive-compulsive behaviors (PC4). These principal components were associated with spatially segregated fiber tracts linking the subthalamic region and frontal cortices (i.e., with fiber tract profiles peaking in different locations; see also unthresholded fiber tract profiles available as Figure S2). The positive and negative fiber tracts are displayed in (B) for each of the PCs (positive fibers in the respective color, and negative fibers in white), while (D) shows all positive fiber tracts together (view from postero-superior). (C) illustrates the correlation between empirical PC scores and PC scores as estimated based on the overlap of E-fields with the tracts.

in impulsive-compulsive behaviors to those of empathy (hereafter referred to as improvement of empathy and worsening in impulsive-compulsive behaviors). There was no statistically significant correlation between LEDD reduction and PC2, PC3, or PC4 scores (all $ps > 0.5$).
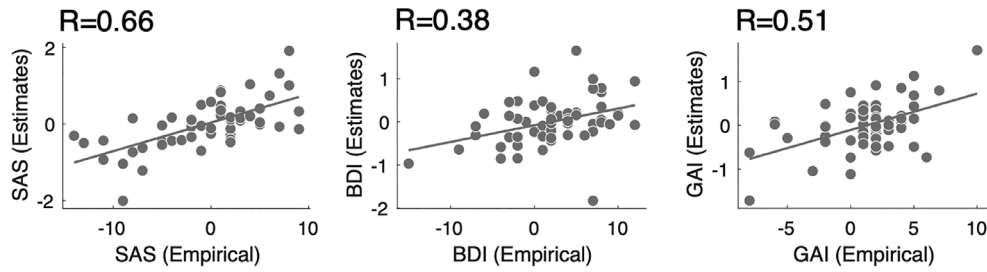
3.3 | Structural Connectivity

The four principal components were associated with spatially segregated fiber tracts linking the subthalamic region and frontal cortices (i.e., with fiber tracts profiles peaking in different locations; Figure 3 and Figure S4). The unthresholded fiber profiles are shown in Figure S2. Correlation coefficients between empirical and estimated PC scores were $R = 0.66$ (PC1), $R = 0.66$ (PC2), $R = 0.57$ (PC3), and $R = 0.51$ (PC4), respectively. Of note, all estimates were derived in a circular fashion, meaning that the same patients were used to build the model and obtain estimates. We hence refrain from reporting p-values. As a first observation, the extent of modulation of these four tracts was able to account for improvements in individual scores. This means that it was possible to "store" improvements along a large battery of scores onto a lower-dimensional set of anatomical tracts and to "retrieve" the high-dimensional score data again merely

from how strongly the tracts were modulated (by "unmixing" the PCA that led to the creation of tracts). This could be achieved even though the four retained PCs only explained 67% of the variance. Specifically, correlation coefficients between empirical and estimated outcomes ranged from $R = 0.38$ to $R = 0.66$ (SAS: $R = 0.66$; BDI: $R = 0.38$; GAI: $R = 0.51$; QUIP-RS: $R = 0.57$; BIS-11 attentional: $R = 0.52$; BIS-11 motor: $R = 0.48$; BIS-11 non-planning: $R = 0.60$; EQ: $R = 0.49$; MoCA: $R = 0.48$; MMSE: $R = 0.41$; Figure 4). Table S5 shows how these values compare to those obtained using a "score-by-score" standard fiber filtering approach. Figure S5 shows significant fiber tracts at $p < 0.05$ (uncorrected). Cross-validation of these results (5-fold, 10-fold, and leave-one-out) did not reach statistical significance, with the exception of SAS in the 5-fold and leave-one-out designs (5-fold: $R = 0.26$, $p = 0.05$; 10-fold: $R = 0.25$, $p = 0.06$; leave-one-out: $R = 0.26$, $p = 0.04$; all other p-values > 0.1). Fiber tracts are available as an "atlas" as part of the Lead-DBS software.
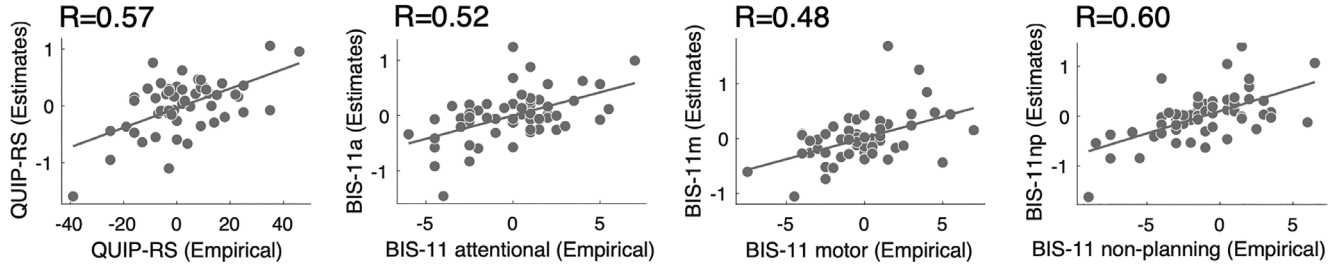
3.4 | Out-of-Sample Validation

The validation cohort consisted of 68 PD patients with bilateral STN-DBS (28 females, 40 males, age at surgery: 61.7 ± 9.0 years; Table 2). Electrode and active contact positions are shown in
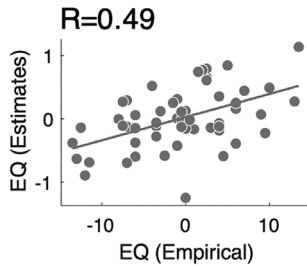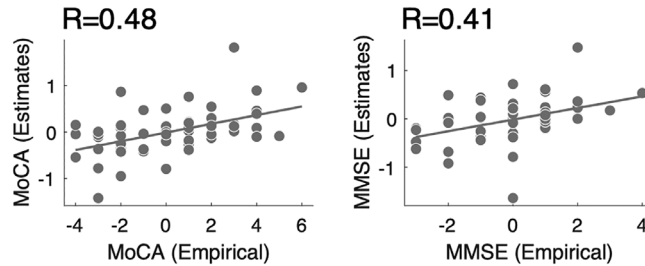
FIGURE 4 | Estimation of the individual score outcomes. Correlations between estimated and empirical outcomes for each of the 10 clinical scores. Estimates of outcomes were derived based on the four-tract model. Because these estimates were derived in a circular fashion (see text for detail), we refrain from reporting *p*-values.

Figure S3. In this independent cohort, there was a weak but statistically significant rank correlation between BDI improvement estimated based on the four-tract model and empirical BDI improvement ($R_{\text{Spearman}} = 0.26$, $p = 0.032$; Figure 5).

4 | Discussion

In this study, we used a novel approach to identify the main dimensions of neuropsychiatric and neuropsychological outcomes of STN-DBS, as well as structural connections whose stimulation was associated with changes along these dimensions. This led to a set of four fiber tracts—one mapping to each of the four principal components—which would all be stimulated to varying degrees by most electrodes. Exactly this weighted mix of how these tracts were stimulated could be used to map back to estimates of improvements along the original 10 clinical scores. In an independent cohort, the combination of tracts stimulated was able to explain significant amounts of variance in depression outcomes. While our study could not be expected to yield a robust and generalizable predictive model of DBS outcomes, it can be seen as a proof-of-concept for the proposed methodological approach aiming at projecting a high-dimensional score battery onto a low-dimensional architecture of tracts, only to

expand results to estimate changes within the high-dimensional score battery again.

There are a few key conclusions that may be drawn from this study. First, the dimensionality of the clinical assessment battery could be reduced to four PCs, while explaining sufficient variance (at the behavioral level). Second, these PCs could be associated with spatially segregated fiber tracts linking the subthalamic region and frontal cortices (i.e., with fiber tract profiles peaking in different locations). Importantly, interpreting these PCs and the anatomy of associated tracts may not be straightforward. PCA strives to compress most of the information contained within the initial variables into the first components, and these may not necessarily map onto meaningful correlates in the human brain. This being said, the tracts we identified are still broadly consistent with current knowledge of the networks associated with non-motor effects of DBS (Table S6).

Namely, the first PC could be interpreted as reflecting general non-motor improvement. While showing a left-hemispheric dominance, fibers that were most strongly positively associated with PC1 projected from premotor and supplementary motor regions to the STN on both hemispheres. Stimulation of fibers connecting the associative territory of the left STN to more anterior
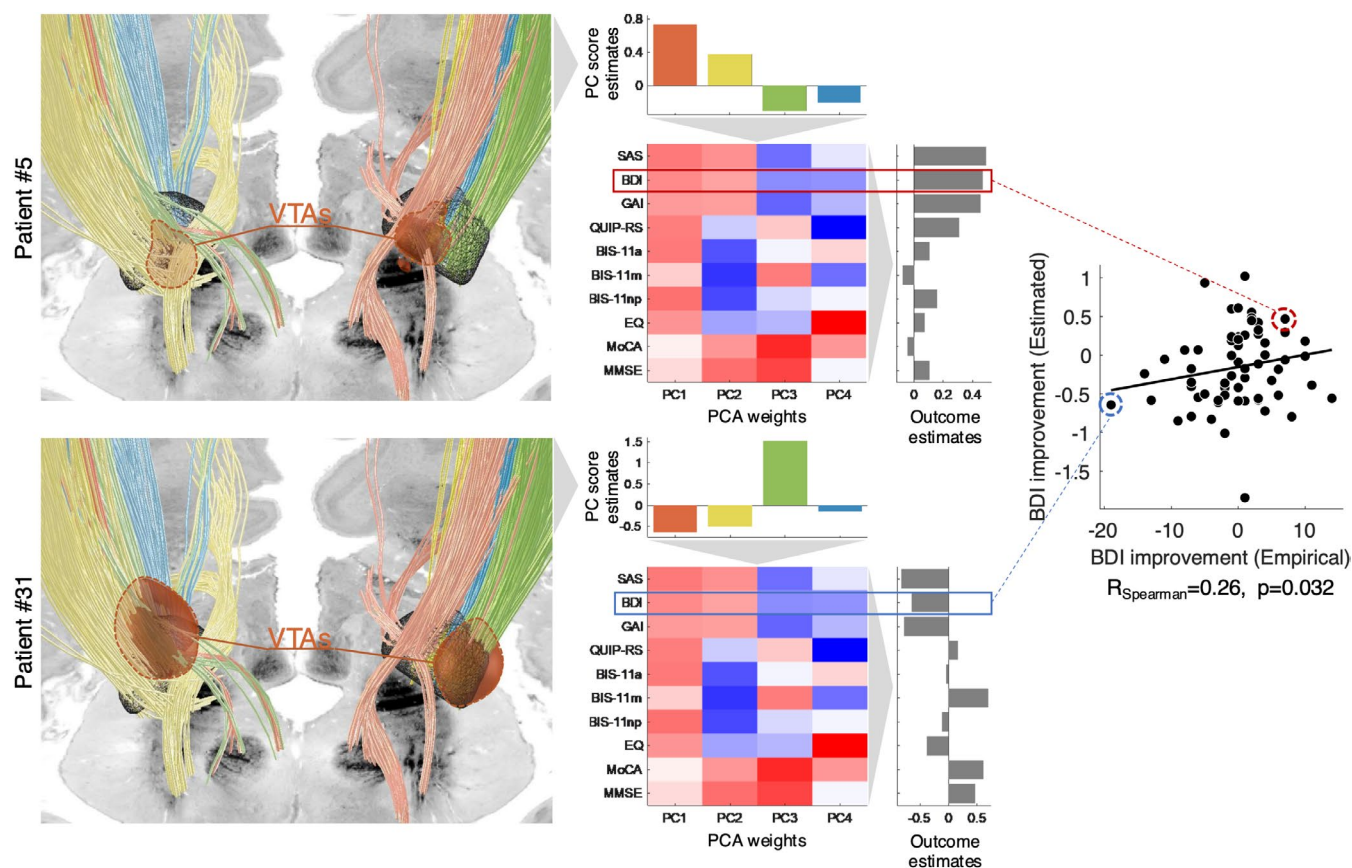
FIGURE 5 | Out-of-sample validation of the four-tract model. An independent cohort of 68 PD patients with bilateral STN-DBS and depression assessment (BDI) was used as a validation cohort. The procedure used to derive estimates of depression outcomes based on the four-tract model is illustrated for two example patients (top and bottom rows). Estimates of PC scores were first obtained based on the overlap of E-fields with the previously identified fiber tracts. Note that volumes of tissue activated (VTAs) are used for visualization only, while unthresholded E-fields were used for analysis (see Section 2). Then, the estimates of PC scores were multiplied with PCA weights to obtain estimates of individual symptom outcomes. Across all patients, the rank correlation between estimated and empirical BDI improvements was weak but statistically significant.

frontal areas was negatively associated with PC1 scores. The positive fibers correspond to the connectivity profile of a well-placed electrode targeting the dorsolateral aspect of the STN (Middlebrooks et al. 2020) and, as such, are consistent with what previous studies have identified as the connectivity profile associated with optimal motor outcomes of STN-DBS for PD (Akram et al. 2017; Horn et al. 2017; Figure S6), as well as improvements in quality of life (Tödt et al. 2022). Altogether, this suggests that PC1 may further represent an overall favorable outcome of surgery, which would be related -at least in part- to well-placed electrodes and stimulation of the dorsolateral aspect of the STN. Unfortunately, UPDRS-III assessments off medication were not available in this cohort, thus the involvement of motor improvement in turn mediating general non-motor improvement could not be directly tested. Indirectly, however, the positive correlation between PC1 scores and LEDD reduction is consistent with this interpretation, since sufficient control of motor symptoms by DBS may have allowed for stronger reductions of dopaminergic treatment.

We interpreted PC2 as representing improvements in mood and cognition and worsening of trait impulsivity. Fibers most strongly associated with this PC were found in the right hemisphere, with weaker associations and lesser segregation in the left hemisphere. Specifically, stimulation of fibers connecting the limbic and associative territories of the right STN to superior, middle, and inferior frontal gyri, as well as the ventromedial prefrontal cortex, was positively associated with PC2 scores, while stimulation of fibers connecting the right STN to motor regions was negatively associated with PC2 scores. This means that modulation of the associative and/or limbic loop in the right hemisphere was associated with better mood and cognition outcomes, but worse impulsivity outcomes, consistent with previous studies linking modulation of this loop with postoperative mania or impulsivity (Mosley et al. 2018; Mosley, Paliwal, et al. 2020; Prange et al. 2022), as well as improved apathy (Béreau et al. 2023).

PC3 mainly represented improvements in cognition. Tracts associated with this tract showed a more symmetric pattern, despite stronger associations in the right hemisphere. Specifically, a gradient was seen along the main axis of the STN such that stimulation of fibers linking its posterolateral aspect to the primary motor, premotor, and supplementary motor cortices was positively associated with PC3 scores, while stimulation of tracts connecting its anteromedial aspect to more anterior frontal areas was negatively associated with PC3 scores. This is in direct agreement with a recent study that found stimulation of the anteroventral aspect of the STN to be associated with cognitive decline (Reich et al. 2022; see also Witt et al. 2013). Interestingly, in the same study,

reprogramming stimulation to avoid this region of the STN improved cognition in a prospective patient case (Reich et al. 2022).

Finally, PC4 represented improvements in empathy and worsening of impulsive-compulsive behaviors. While the opposite loadings of these symptoms may sound surprising at first (Mosley, Robinson, et al. 2019), one should remember that PC4 only accounts for part of the variance in these symptoms; indeed, the two corresponding variables were not strongly negatively correlated ($R = -0.02$; Table S1). Still, this component remains more difficult to interpret than the others (and obviously explained the least amount of variance across the four retained PCs). Connectivity results showed that fibers positively associated with PC4 scores reached more anterior and lateral aspects of the STN, and mostly connected to superior and middle frontal cortices, while fibers negatively associated with PC4 scores reached more posterior and medial aspects of the STN.

Beyond tract anatomy and the four identified components, a key finding of this study is that the four-tract model could be used to estimate individual symptom outcomes both in the original sample as well as in an independent validation cohort (although only a single symptom was available in the validation cohort). This illustrates the potential value of the proposed approach. Indeed, multiple situations may exist where a wide range of DBS responses needs to be mapped onto the local anatomy of the brain (Béreau et al. 2023; Kratter et al. 2022; Mosley, Paliwal, et al. 2019; Petry-Schmelzer et al. 2019; Tödt et al. 2022). In prior work, this was done "score-by-score," i.e., each individual score was mapped to a local or tract surrogate to study its response to DBS (Petry-Schmelzer et al. 2019). Here, we propose to map in an N to T fashion, where N (number of scores) may be larger than T (number of tracts, or fiber bundles). We introduce openly available code and software to encode high-dimensional data (N) to low-dimensional tract model (T) in this fashion, and to "retrieve" information back from the encoded set of tracts to estimate changes in high-dimensional (N) space. We envision that such low-dimensional tract models may be used to inform DBS programming and improve patients' outcomes. Importantly, the fact that well-segregated tracts were associated with different dimensions of non-motor outcomes suggests that it may not be possible to find settings that would improve each and every single symptom. Hence, a "one-size-fits-all" approach may not be appropriate; rather, programming could be personalized in order to address the main symptoms of concern in individual patients (Hollunder et al. 2022; Siddiqi et al. 2020). Alternatively, and additionally, novel lead designs with up to 16 contacts may make it possible to modulate several networks simultaneously using a single well-placed electrode (Rajamani et al. 2024). Overall, automated DBS programming algorithms are a pressing need given the ongoing complexification of electrode designs, which renders the exploration of the parameter space through monopolar review impractical (Anderson et al. 2018; Frey et al. 2022; Krauss et al. 2021; Roediger et al. 2022, 2023). These algorithms may be especially useful for symptoms that do not respond rapidly to changes in stimulation parameters, in contrast to cardinal symptoms of PD. Our group has recently published an algorithm that could be used to suggest optimal DBS stimulation parameters for a given patient's needs based on tract landscapes such as the present one (Rajamani et al. 2024). Yet, challenges remain. We note that accurate prediction of

clinical outcomes for the out-of-sample cohort could not be achieved in the present study (and cross-validation within the main cohort was mostly non-significant). Rather, our model could only explain statistically significant amounts of variance in outcome ranks. One might argue that estimating ranks may be enough to choose from a finite set of different DBS settings for a given patient (Rajamani et al. 2024). Still, we believe that much larger sample sizes would be required to build a model capable of clinically relevant predictions. Moreover, our model can only explain the part of the variance in clinical outcomes that is (directly or indirectly) associated with stimulation itself. While this makes sense from the perspective of informing DBS programming algorithms, ultimately, proper predictive models of non-motor outcomes of STN-DBS may require the inclusion of other variables such as baseline patient characteristics, comorbidities, age, and disease subtype. Further, non-motor outcomes may be improved by other means above and beyond DBS, such as management of dopaminergic treatment, or selection of patients most likely to maximally benefit from DBS (Czernecki et al. 2008; Rossi et al. 2018; Weiss et al. 2021).

Beyond PD, our approach may be valuable for psychiatric disorders. These disorders are characterized by important symptomatic and neurobiological heterogeneity as well as comorbidity, which prompted suggestions to focus on core behavioral or cognitive dimensions of impairment that span across traditional diagnostic boundaries and map onto distinct dysfunctional circuits (Cuthbert and Insel 2013; Figee and Mayberg 2021; Fiore et al. 2023; Insel et al. 2010; Robbins et al. 2012; Widge 2023; Widge et al. 2017). Our method may be used to reduce large clinical assessment batteries to a low number of dimensions and map those to segregated circuits in a data-driven fashion.

Our study is not exempt from limitations. While the presence of asymmetries in the associations between PC scores and fiber tracts is not surprising given the known lateralization of certain neuropsychiatric symptoms such as depression (George et al. 1994; see also Table S6), spurious asymmetries cannot be ruled out completely, and optimally, our findings should be replicated before definitive conclusions are drawn. Although we used well-established criteria to determine how many PCs to retain, retaining four PCs resulted in explaining only 67% of the variance, which limited the potential predictive value of the model. Moreover, our results are very much dependent upon the PCA solution accurately capturing the correlation structure of the clinical assessments. Our study was based on a cohort of 56 patients only, with an additional 68 patients for validation. As stated above, larger and more heterogeneous samples are likely required to achieve a stable, accurate PCA solution and develop clinically useful models. We note that data from large, well-characterized multicenter cohorts is being increasingly collected (e.g., by the Movement Disorder Society non-motor PD and PREDI-STIM study groups), such that this may be achievable in the near future. Future models may also include symptoms that were not well represented in the present assessment battery. This includes UPDRS-III scores in the off-medication state, which were not available and could not be accounted for in the present model. Moreover, external validation could only be performed for a single score (i.e., depression). Given these limitations, our study should be considered as a proof-of-concept, and the model itself should not be overinterpreted. In other words, in our view,

the present model does not represent a final answer, and future studies should extend this work to build a more robust and comprehensive predictive model of non-motor outcome of STN-DBS. Other methodological limitations include inherent imprecision in electrode localizations due to co-registration and normalization of the images despite the use of a dedicated pipeline (Ewert et al. 2019; Horn et al. 2019; Neudorfer et al. 2023), unavoidable uncertainty in the estimation of the stimulated area through E-field modeling (Duffley et al. 2019), and use of normative connectomes, which may not accurately represent individual patient anatomy (but see Horn and Fox 2020; Wang et al. 2021).

In conclusion, we propose a novel approach aimed at mapping changes along extensive clinical score batteries to the modulation of a small number of fiber bundles in the human brain. Such tracts might be used to predict and improve DBS outcomes, paving the way for treatment personalization. This approach may prove valuable not only in PD, but also in psychiatric disorders where patients usually present with comorbid symptoms that may in part rely on shared dysfunctional brain circuits. By helping identify these circuits, our approach may also contribute toward the comprehensive delineation of what has recently been termed the "dysfunctome" (Hollunder et al. 2024), i.e., a library of dysfunctional circuits whose neuromodulation was associated with treatment benefit.

References

Abbes, M., E. Lhommée, S. Thobois, et al. 2018. "Subthalamic Stimulation and Neuropsychiatric Symptoms in Parkinson's Disease: Results From a Long-Term Follow-Up Cohort Study." *Journal of Neurology, Neurosurgery, and Psychiatry* 89, no. 8: 836–843. https://doi.org/10.1136/jnnp-2017-316373.

Akram, H., S. N. Sotiropoulos, S. Jbabdi, et al. 2017. "Subthalamic Deep Brain Stimulation Sweet Spots and Hyperdirect Cortical Connectivity in Parkinson's Disease." *NeuroImage* 158: 332–345. https://doi.org/10.1016/j.neuroimage.2017.07.012.

Amunts, K., C. Lepage, L. Borgeat, et al. 2013. "BigBrain: An Ultrahigh-Resolution 3D Human Brain Model." *Science* 340, no. 6139: 1472–1475. https://doi.org/10.1126/science.1235381.

Anderson, D. N., B. Osting, J. Vorwerk, A. D. Dorval, and C. R. Butson. 2018. "Optimized Programming Algorithm for Cylindrical and Directional Deep Brain Stimulation Electrodes." *Journal of Neural Engineering* 15, no. 2: 026005. https://doi.org/10.1088/1741-2552/aaa14b.

Antonini, A., P. Barone, R. Marconi, et al. 2012. "The Progression of Non-Motor Symptoms in Parkinson's Disease and Their Contribution to Motor Disability and Quality of Life." *Journal of Neurology* 259, no. 12: 2621–2631. https://doi.org/10.1007/s00415-012-6557-8.

Åström, M., E. Diczfalusy, H. Martens, and K. Wårdell. 2015. "Relationship Between Neural Activation and Electric Field Distribution During Deep Brain Stimulation." *IEEE Transactions on Biomedical Engineering* 62, no. 2: 664–672. https://doi.org/10.1109/TBME.2014.2363494.

Avants, B. B., N. J. Tustison, G. Song, P. A. Cook, A. Klein, and J. C. Gee. 2011. "A Reproducible Evaluation of ANTs Similarity Metric Performance in Brain Image Registration." *NeuroImage* 54, no. 3: 2033–2044. https://doi.org/10.1016/j.neuroimage.2010.09.025.

Baldermann, J. C., C. Melzer, A. Zapf, et al. 2019. "Connectivity Profile Predictive of Effective Deep Brain Stimulation in Obsessive-Compulsive Disorder." *Biological Psychiatry* 85, no. 9: 735–743. https://doi.org/10.1016/j.biopsych.2018.12.019.

Baron-Cohen, S., and S. Wheelwright. 2004. "The Empathy Quotient: An Investigation of Adults With Asperger Syndrome or High Functioning Autism, and Normal Sex Differences." *Journal of Autism and Developmental Disorders* 34, no. 2: 163–175. https://doi.org/10.1023/b:jadd.0000022607.19833.00.

Barone, P., A. Antonini, C. Colosimo, et al. 2009. "The PRIAMO Study: A Multicenter Assessment of Nonmotor Symptoms and Their Impact on Quality of Life in Parkinson's Disease." *Movement Disorders: Official Journal of the Movement Disorder Society* 24, no. 11: 1641–1649. https://doi.org/10.1002/mds.22643.

Beck, A. T., C. H. Ward, M. Mendelson, J. Mock, and J. Erbaugh. 1961. "An Inventory for Measuring Depression." *Archives of General Psychiatry* 4: 561–571. https://doi.org/10.1001/archpsyc.1961.01710120031004.

Bejjani, B. P., P. Damier, I. Arnulf, et al. 1999. "Transient Acute Depression Induced by High-Frequency Deep-Brain Stimulation." *New England Journal of Medicine* 340, no. 19: 1476–1480. https://doi.org/10.1056/NEJM199905133401905.

Béreau, M., A. Kibleur, M. Servant, et al. 2023. "Motivational and Cognitive Predictors of Apathy After Subthalamic Nucleus Stimulation in Parkinson's Disease." *Brain: A Journal of Neurology* 147, no. 2: awad324. https://doi.org/10.1093/brain/awad324.

Burgess, P. W., and T. Shallice. 1997. *The Hayling and Brixton Tests.* Thames Valley Test Company.

Butenko, K., C. Bahls, M. Schröder, R. Köhling, and U. Van Rienen. 2020. "OSS-DBS: Open-Source Simulation Platform for Deep Brain Stimulation With a Comprehensive Automated Modeling." *PLoS*

Computational Biology 16, no. 7: e1008023. https://doi.org/10.1371/journal.pcbi.1008023.

Castelli, L., P. Perozzo, M. Zibetti, et al. 2006. "Chronic Deep Brain Stimulation of the Subthalamic Nucleus for Parkinson's Disease: Effects on Cognition, Mood, Anxiety and Personality Traits." *European Neurology* 55, no. 3: 136–144. https://doi.org/10.1159/000093213.

Castrioto, A., E. Lhommée, E. Moro, and P. Krack. 2014. "Mood and Behavioural Effects of Subthalamic Stimulation in Parkinson's Disease." *Lancet Neurology* 13, no. 3: 287–305. https://doi.org/10.1016/S1474-4422(13)70294-1.

Cuthbert, B. N., and T. R. Insel. 2013. "Toward the Future of Psychiatric Diagnosis: The Seven Pillars of RDoC." *BMC Medicine* 11: 126. https://doi.org/10.1186/1741-7015-11-126.

Czernecki, V., M. Schüpbach, S. Yaici, et al. 2008. "Apathy Following Subthalamic Stimulation in Parkinson Disease: A Dopamine Responsive Symptom." *Movement Disorders: Official Journal of the Movement Disorder Society* 23, no. 7: 964–969. https://doi.org/10.1002/mds.21949.

Dafsari, H. S., P. Reddy, C. Herchenbach, et al. 2016. "Beneficial Effects of Bilateral Subthalamic Stimulation on Non-Motor Symptoms in Parkinson's Disease." *Brain Stimulation* 9, no. 1: 78–85. https://doi.org/10.1016/j.brs.2015.08.005.

Dembek, T. A., A. Hellerbach, H. Jergas, et al. 2021. "DiODe v2: Unambiguous and Fully-Automated Detection of Directional DBS Lead Orientation." *Brain Sciences* 11, no. 11: 1450. https://doi.org/10.3390/brainsci11111450.

Deuschl, G., C. Schade-Brittinger, P. Krack, et al. 2006. "A Randomized Trial of Deep-Brain Stimulation for Parkinson's Disease." *New England Journal of Medicine* 355, no. 9: 896–908. https://doi.org/10.1056/NEJMoa060281.

Duffley, G., D. N. Anderson, J. Vorwerk, A. D. Dorval, and C. R. Butson. 2019. "Evaluation of Methodologies for Computing the Deep Brain Stimulation Volume of Tissue Activated." *Journal of Neural Engineering* 16, no. 6: 066024. https://doi.org/10.1088/1741-2552/ab3c95.

Emmi, A., A. Antonini, V. Macchi, A. Porzionato, and R. Caro. 2020. "Anatomy and Connectivity of the Subthalamic Nucleus in Humans and Non-Human Primates." *Frontiers in Neuroanatomy* 14: 13. https://doi.org/10.3389/fnana.2020.00013.

Emre, M., D. Aarsland, R. Brown, et al. 2007. "Clinical Diagnostic Criteria for Dementia Associated With Parkinson's Disease." *Movement Disorders: Official Journal of the Movement Disorder Society* 22, no. 12: 1689–1707; quiz 1837. https://doi.org/10.1002/mds.21507.

Ewert, S., A. Horn, F. Finkel, N. Li, A. A. Kühn, and T. M. Herrington. 2019. "Optimization and Comparative Evaluation of Nonlinear Deformation Algorithms for Atlas-Based Segmentation of DBS Target Nuclei." *NeuroImage* 184: 586–598. https://doi.org/10.1016/j.neuroimage.2018.09.061.

Ewert, S., P. Plettig, N. Li, et al. 2018. "Toward Defining Deep Brain Stimulation Targets in MNI Space: A Subcortical Atlas Based on Multimodal MRI, Histology and Structural Connectivity." *NeuroImage* 170: 271–282. https://doi.org/10.1016/j.neuroimage.2017.05.015.

Fasano, A., A. Daniele, and A. Albanese. 2012. "Treatment of Motor and Non-Motor Features of Parkinson's Disease With Deep Brain Stimulation." *Lancet Neurology* 11, no. 5: 429–442. https://doi.org/10.1016/S1474-4422(12)70049-2.

Figee, M., and H. Mayberg. 2021. "The Future of Personalized Brain Stimulation." *Nature Medicine* 27, no. 2: 196–197. https://doi.org/10.1038/s41591-021-01243-7.

Fiore, V. G., A. H. Smith, and M. Figee. 2023. "Toward Personalized Deep Brain Stimulation for Obsessive-Compulsive Disorder." *Biological Psychiatry: Cognitive Neuroscience and Neuroimaging* 8, no. 3: 235–237. https://doi.org/10.1016/j.bpsc.2023.01.004.

Floden, D., S. E. Cooper, S. D. Griffith, and A. G. Machado. 2014. "Predicting Quality of Life Outcomes After Subthalamic Nucleus Deep Brain Stimulation." *Neurology* 83, no. 18: 1627–1633. https://doi.org/10.1212/WNL.0000000000000943.

Folstein, M. F., S. E. Folstein, and P. R. McHugh. 1975. "'Mini-Mental State'. A Practical Method for Grading the Cognitive State of Patients for the Clinician." *Journal of Psychiatric Research* 12, no. 3: 189–198. https://doi.org/10.1016/0022-3956(75)90026-6.

Frey, J., J. Cagle, K. Johnson, et al. 2022. "Past, Present, and Future of Deep Brain Stimulation: Hardware, Software, Imaging, Physiology and Novel Approaches." *Frontiers in Neurology* 13: 825178. https://doi.org/10.3389/fneur.2022.825178.

Friston, K., J. Ashburner, S. Kiebel, T. Nichols, and W. Penny, eds. 2007. *Statistical Parametric Mapping.* Academic Press. https://doi.org/10.1016/B978-0-12-372560-8.50052-8.

Gadot, R., N. Li, B. Shofty, et al. 2024. "Tractography-Based Modeling Explains Treatment Outcomes in Patients Undergoing Deep Brain Stimulation for Obsessive-Compulsive Disorder." *Biological Psychiatry* 96, no. 2: 95–100. https://doi.org/10.1016/j.biopsych.2023.01.017.

George, M. S., T. A. Ketter, and R. M. Post. 1994. "Prefrontal Cortex Dysfunction in Clinical Depression." *Depression* 2, no. 2: 59–72. https://doi.org/10.1002/depr.3050020202.

Haynes, W. I. A., and S. N. Haber. 2013. "The Organization of Prefrontal-Subthalamic Inputs in Primates Provides an Anatomical Substrate for Both Functional Specificity and Integration: Implications for Basal Ganglia Models and Deep Brain Stimulation." *Journal of Neuroscience: The Official Journal of the Society for Neuroscience* 33, no. 11: 4804–4814. https://doi.org/10.1523/JNEUROSCI.4674-12.2013.

Hollunder, B., J. L. Ostrem, I. A. Sahin, et al. 2024. "Mapping Dysfunctional Circuits in the Frontal Cortex Using Deep Brain Stimulation." *Nature Neuroscience* 27, no. 3: 573–586. https://doi.org/10.1038/s41593-024-01570-1.

Hollunder, B., N. Rajamani, S. H. Siddiqi, et al. 2022. "Toward Personalized Medicine in Connectomic Deep Brain Stimulation." *Progress in Neurobiology* 210: 102211. https://doi.org/10.1016/j.pneurobio.2021.102211.

Horn, A., and M. Fox. 2020. "Opportunities of Connectomic Neuromodulation." *NeuroImage* 221: 117180. https://doi.org/10.1016/j.neuroimage.2020.117180.

Horn, A., and A. A. Kühn. 2015. "Lead-DBS: A Toolbox for Deep Brain Stimulation Electrode Localizations and Visualizations." *NeuroImage* 107: 127–135. https://doi.org/10.1016/j.neuroimage.2014.12.002.

Horn, A., N. Li, T. Dembek, et al. 2019. "Lead-DBS v2: Towards a Comprehensive Pipeline for Deep Brain Stimulation Imaging." *NeuroImage* 184: 293–316. https://doi.org/10.1016/j.neuroimage.2018.08.068.

Horn, A., M. Reich, J. Vorwerk, et al. 2017. "Connectivity Predicts Deep Brain Stimulation Outcome in Parkinson Disease." *Annals of Neurology* 82, no. 1: 67–78. https://doi.org/10.1002/ana.24974.

Horn, A., M. M. Reich, S. Ewert, et al. 2022. "Optimal Deep Brain Stimulation Sites and Networks for Cervical vs. Generalized Dystonia." *Proceedings of the National Academy of Sciences of the United States of America* 119, no. 14: e2114985119. https://doi.org/10.1073/pnas.2114985119.

Hughes, A. J., S. E. Daniel, L. Kilford, and A. J. Lees. 1992. "Accuracy of Clinical Diagnosis of Idiopathic Parkinson's Disease: A Clinico-Pathological Study of 100 Cases." *Journal of Neurology, Neurosurgery, and Psychiatry* 55, no. 3: 181–184. https://doi.org/10.1136/jnnp.55.3.181.

Husch, A., V. Petersen, M. Gemmar, J. Goncalves, and F. Hertel. 2018. "PaCER—A Fully Automated Method for Electrode Trajectory and Contact Reconstruction in Deep Brain Stimulation." *NeuroImage: Clinical* 17: 80–89. https://doi.org/10.1016/j.nicl.2017.10.004.

Insel, T., B. Cuthbert, M. Garvey, et al. 2010. "Research Domain Criteria (RDoC): Toward a New Classification Framework for Research on Mental Disorders." *American Journal of Psychiatry* 167, no. 7: 748–751. https://doi.org/10.1176/appi.ajp.2010.09091379.

Irmen, F., A. Horn, P. Mosley, et al. 2020. "Left Prefrontal Connectivity Links Subthalamic Stimulation With Depressive Symptoms." *Annals of Neurology* 87, no. 6: 962–975. https://doi.org/10.1002/ana.25734.

Kim, A., Y. E. Kim, H.-J. Kim, et al. 2018. "A 7-Year Observation of the Effect of Subthalamic Deep Brain Stimulation on Impulse Control Disorder in Patients With Parkinson's Disease." *Parkinsonism & Related Disorders* 56: 3–8. https://doi.org/10.1016/j.parkreldis.2018.07.010.

Kirby, K. N., N. M. Petry, and W. K. Bickel. 1999. "Heroin Addicts Have Higher Discount Rates for Delayed Rewards Than Non-Drug-Using Controls." *Journal of Experimental Psychology. General* 128, no. 1: 78–87. https://doi.org/10.1037/0096-3445.128.1.78.

Kleiner-Fisman, G., J. Herzog, D. N. Fisman, et al. 2006. "Subthalamic Nucleus Deep Brain Stimulation: Summary and Meta-Analysis of Outcomes." *Movement Disorders: Official Journal of the Movement Disorder Society* 21, no. Suppl 14: S290–S304. https://doi.org/10.1002/mds.20962.

Kratter, I. H., A. Jorge, M. T. Feyder, et al. 2022. "Depression History Modulates Effects of Subthalamic Nucleus Topography on Neuropsychological Outcomes of Deep Brain Stimulation for Parkinson's Disease." *Translational Psychiatry* 12, no. 1: 213. https://doi.org/10.1038/s41398-022-01978-y.

Krauss, J. K., N. Lipsman, T. Aziz, et al. 2021. "Technology of Deep Brain Stimulation: Current Status and Future Directions." *Nature Reviews. Neurology* 17, no. 2: 75–87. https://doi.org/10.1038/s41582-020-00426-z.

Lhommée, E., L. Wojtecki, V. Czernecki, et al. 2018. "Behavioural Outcomes of Subthalamic Stimulation and Medical Therapy Versus Medical Therapy Alone for Parkinson's Disease With Early Motor Complications (EARLYSTIM Trial): Secondary Analysis of an Open-Label Randomised Trial." *Lancet Neurology* 17, no. 3: 223–231. https://doi.org/10.1016/S1474-4422(18)30035-8.

Li, N., J. C. Baldermann, A. Kibleur, et al. 2020. "A Unified Connectomic Target for Deep Brain Stimulation in Obsessive-Compulsive Disorder." *Nature Communications* 11, no. 1: 3364. https://doi.org/10.1038/s41467-020-16734-3.

Lozano, A. M., N. Lipsman, H. Bergman, et al. 2019. "Deep Brain Stimulation: Current Challenges and Future Directions." *Nature Reviews Neurology* 15, no. 3: 148–160. https://doi.org/10.1038/s41582-018-0128-2.

Martinez-Martin, P. 2011. "The Importance of Non-Motor Disturbances to Quality of Life in Parkinson's Disease." *Journal of the Neurological Sciences* 310, no. 1–2: 12–16. https://doi.org/10.1016/j.jns.2011.05.006.

Martinez-Martin, P., C. Rodriguez-Blazquez, K. Abe, et al. 2009. "International Study on the Psychometric Attributes of the Non-Motor Symptoms Scale in Parkinson Disease." *Neurology* 73, no. 19: 1584–1591. https://doi.org/10.1212/WNL.0b013e3181c0d416.

Middlebrooks, E. H., R. A. Domingo, T. Vivas-Buitrago, et al. 2020. "Neuroimaging Advances in Deep Brain Stimulation: Review of Indications, Anatomy, and Brain Connectomics." *American Journal of Neuroradiology* 41, no. 9: 1558–1568. https://doi.org/10.3174/ajnr.A6693.

Mosley, P. E., S. Paliwal, K. Robinson, et al. 2019. "The Structural Connectivity of Discrete Networks Underlies Impulsivity and Gambling in Parkinson's Disease." *Brain* 142, no. 12: 3917–3935. https://doi.org/10.1093/brain/awz327.

Mosley, P. E., S. Paliwal, K. Robinson, et al. 2020. "The Structural Connectivity of Subthalamic Deep Brain Stimulation Correlates With Impulsivity in Parkinson's." *Brain: A Journal of Neurology* 143, no. 7: 2235–2254. https://doi.org/10.1093/brain/awaa148.

Mosley, P. E., K. Robinson, T. Coyne, et al. 2020. "Subthalamic Deep Brain Stimulation Identifies Frontal Networks Supporting Initiation, Inhibition and Strategy Use in Parkinson's Disease: Initiation and Inhibition After STN-DBS for PD." *NeuroImage* 223: 117352. https://doi.org/10.1016/j.neuroimage.2020.117352.

Mosley, P. E., K. Robinson, T. Coyne, P. Silburn, M. Breakspear, and A. Carter. 2019. "'Woe Betides Anybody Who Tries to Turn Me Down'. A Qualitative Analysis of Neuropsychiatric Symptoms Following Subthalamic Deep Brain Stimulation for Parkinson's Disease." *Neuroethics* 14, no. S1: 47–63. https://doi.org/10.1007/s12152-019-09410-x.

Mosley, P. E., D. Smith, T. Coyne, P. Silburn, M. Breakspear, and A. Perry. 2018. "The Site of Stimulation Moderates Neuropsychiatric Symptoms After Subthalamic Deep Brain Stimulation for Parkinson's Disease." *NeuroImage. Clinical* 18: 996–1006. https://doi.org/10.1016/j.nicl.2018.03.009.

Nasreddine, Z. S., N. A. Phillips, V. Bédirian, et al. 2005. "The Montreal Cognitive Assessment, MoCA: A Brief Screening Tool for Mild Cognitive Impairment." *Journal of the American Geriatrics Society* 53, no. 4: 695–699. https://doi.org/10.1111/j.1532-5415.2005.53221.x.

Neudorfer, C., K. Butenko, S. Oxenford, et al. 2023. "Lead-DBS v3.0: Mapping Deep Brain Stimulation Effects to Local Anatomy and Global Networks." *NeuroImage* 268: 119862. https://doi.org/10.1016/j.neuroimage.2023.119862.

Oxenford, S., A. S. Ríos, B. Hollunder, et al. 2024. "WarpDrive: Improving Spatial Normalization Using Manual Refinements." *Medical Image Analysis* 91: 103041. https://doi.org/10.1016/j.media.2023.103041.

Pachana, N. A., G. J. Byrne, H. Siddle, N. Koloski, E. Harley, and E. Arnold. 2007. "Development and Validation of the Geriatric Anxiety Inventory." *International Psychogeriatrics* 19, no. 1: 103–114. https://doi.org/10.1017/S1041610206003504.

Patton, J. H., M. S. Stanford, and E. S. Barratt. 1995. "Factor Structure of the Barratt Impulsiveness Scale." *Journal of Clinical Psychology* 51, no. 6: 768–774.

Petry-Schmelzer, J. N., M. Krause, T. A. Dembek, et al. 2019. "Non-Motor Outcomes Depend on Location of Neurostimulation in Parkinson's Disease." *Brain* 142, no. 11: 3592–3604. https://doi.org/10.1093/brain/awz285.

Prange, S., Z. Lin, M. Nourredine, et al. 2022. "Limbic Stimulation Drives Mania in STN-DBS in Parkinson Disease: A Prospective Study." *Annals of Neurology* 92: 411–417. https://doi.org/10.1002/ana.26434.

Rajamani, N., H. Friedrich, K. Butenko, et al. 2024. "Deep Brain Stimulation of Symptom-Specific Networks in Parkinson's Disease." *Nature Communications* 15, no. 1: 4662. https://doi.org/10.1038/s41467-024-48731-1.

Reich, M. M., J. Hsu, M. Ferguson, et al. 2022. "A Brain Network for Deep Brain Stimulation Induced Cognitive Decline in Parkinson's Disease." *Brain: A Journal of Neurology* 145, no. 4: 1410–1421. https://doi.org/10.1093/brain/awac012.

Reynolds, B., A. Ortengren, J. B. Richards, and H. de Wit. 2006. "Dimensions of Impulsive Behavior: Personality and Behavioral Measures." *Personality and Individual Differences* 40, no. 2: 305–315. https://doi.org/10.1016/j.paid.2005.03.024.

Ríos, A. S., S. Oxenford, C. Neudorfer, et al. 2022. "Optimal Deep Brain Stimulation Sites and Networks for Stimulation of the Fornix in Alzheimer's Disease." *Nature Communications* 13, no. 1: 7707. https://doi.org/10.1038/s41467-022-34510-3.

Robbins, T. W., C. M. Gillan, D. G. Smith, S. de Wit, and K. D. Ersche. 2012. "Neurocognitive Endophenotypes of Impulsivity and Compulsivity: Towards Dimensional Psychiatry." *Trends in Cognitive Sciences* 16, no. 1: 81–91. https://doi.org/10.1016/j.tics.2011.11.009.

Roediger, J., T. A. Dembek, J. Achtzehn, et al. 2023. "Automated Deep Brain Stimulation Programming Based on Electrode Location: A

Randomised, Crossover Trial Using a Data-Driven Algorithm." *Lancet Digital Health* 5, no. 2: e59–e70. https://doi.org/10.1016/S2589-7500(22)00214-X.

Roediger, J., T. A. Dembek, G. Wenzel, K. Butenko, A. A. Kühn, and A. Horn. 2022. "StimFit-A Data-Driven Algorithm for Automated Deep Brain Stimulation Programming." *Movement Disorders: Official Journal of the Movement Disorder Society* 37, no. 3: 574–584. https://doi.org/10.1002/mds.28878.

Rossi, M., V. Bruno, J. Arena, Á. Cammarota, and M. Merello. 2018. "Challenges in PD Patient Management After DBS: A Pragmatic Review." *Movement Disorders Clinical Practice* 5, no. 3: 246–254. https://doi.org/10.1002/mdc3.12592.

Schuepbach, W. M. M., J. Rau, K. Knudsen, et al. 2013. "Neurostimulation for Parkinson's Disease With Early Motor Complications." *New England Journal of Medicine* 368, no. 7: 610–622. https://doi.org/10.1056/NEJMoa1205158.

Shores, E. A., J. R. Carstairs, and J. R. Crawford. 2006. "Excluded Letter Fluency Test (ELF): Norms and Test–Retest Reliability Data for Healthy Young Adults." *Brain Impairment* 7, no. 1: 26–32. https://doi.org/10.1375/brim.7.1.26.

Siddiqi, S. H., S. F. Taylor, D. Cooke, A. Pascual-Leone, M. S. George, and M. D. Fox. 2020. "Distinct Symptom-Specific Treatment Targets for Circuit-Based Neuromodulation." *American Journal of Psychiatry* 177, no. 5: 435–446. https://doi.org/10.1176/appi.ajp.2019.19090915.

Smith, A. H., K. S. Choi, A. C. Waters, et al. 2021. "Replicable Effects of Deep Brain Stimulation for Obsessive-Compulsive Disorder." *Brain Stimulation* 14, no. 1: 1–3. https://doi.org/10.1016/j.brs.2020.10.016.

Starkstein, S. E., H. S. Mayberg, T. J. Preziosi, P. Andrezejewski, R. Leiguarda, and R. G. Robinson. 1992. "Reliability, Validity, and Clinical Correlates of Apathy in Parkinson's Disease." *Journal of Neuropsychiatry and Clinical Neurosciences* 4, no. 2: 134–139. https://doi.org/10.1176/jnp.4.2.134.

Thobois, S., C. Ardouin, E. Lhommée, et al. 2010. "Non-Motor Dopamine Withdrawal Syndrome After Surgery for Parkinson's Disease: Predictors and Underlying Mesolimbic Denervation." *Brain* 133, no. 4: 1111–1127. https://doi.org/10.1093/brain/awq032.

Tödt, I., B. Al-Fatly, O. Granert, et al. 2022. "The Contribution of Subthalamic Nucleus Deep Brain Stimulation to the Improvement in Motor Functions and Quality of Life." *Movement Disorders* 37, no. 2: 291–301. https://doi.org/10.1002/mds.28952.

Van Essen, D. C., K. Ugurbil, E. Auerbach, et al. 2012. "The Human Connectome Project: A Data Acquisition Perspective." *NeuroImage* 62, no. 4: 2222–2231. https://doi.org/10.1016/j.neuroimage.2012.02.018.

Volkmann, J., C. Daniels, and K. Witt. 2010. "Neuropsychiatric Effects of Subthalamic Neurostimulation in Parkinson Disease." *Nature Reviews. Neurology* 6, no. 9: 487–498. https://doi.org/10.1038/nrneurol.2010.111.

Voon, V., C. Kubu, P. Krack, J.-L. Houeto, and A. I. Tröster. 2006. "Deep Brain Stimulation: Neuropsychological and Neuropsychiatric Issues." *Movement Disorders: Official Journal of the Movement Disorder Society* 21, no. Suppl 14: S305–S327. https://doi.org/10.1002/mds.20963.

Wang, Q., H. Akram, M. Muthuraman, et al. 2021. "Normative vs. Patient-Specific Brain Connectivity in Deep Brain Stimulation." *NeuroImage* 224: 117307. https://doi.org/10.1016/j.neuroimage.2020.117307.

Weaver, F. M., K. Follett, M. Stern, et al. 2009. "Bilateral Deep Brain Stimulation vs Best Medical Therapy for Patients With Advanced Parkinson Disease: A Randomized Controlled Trial." *JAMA* 301, no. 1: 63–73. https://doi.org/10.1001/jama.2008.929.

Weintraub, D., J. Koester, M. N. Potenza, et al. 2010. "Impulse Control Disorders in Parkinson Disease: A Cross-Sectional Study of 3090 Patients." *Archives of Neurology* 67, no. 5: 589–595. https://doi.org/10.1001/archneurol.2010.65.

Weintraub, D., E. Mamikonyan, K. Papay, J. A. Shea, S. X. Xie, and A. Siderowf. 2012. "Questionnaire for Impulsive-Compulsive Disorders in Parkinson's Disease–Rating Scale." *Movement Disorders: Official Journal of the Movement Disorder Society* 27, no. 2: 242–247. https://doi.org/10.1002/mds.24023.

Weiss, D., J. Volkmann, A. Fasano, A. Kühn, P. Krack, and G. Deuschl. 2021. "Changing Gears—DBS for Dopaminergic Desensitization in Parkinson's Disease?" *Annals of Neurology* 90: 699–710. https://doi.org/10.1002/ana.26164.

Welter, M.-L., M. Schuepbach, V. Czernecki, et al. 2014. "Optimal Target Localization for Subthalamic Stimulation in Patients With Parkinson Disease." *Neurology* 82, no. 15: 1352–1361. https://doi.org/10.1212/WNL.0000000000000315.

Widge, A. S. 2023. "Closed-Loop Deep Brain Stimulation for Psychiatric Disorders." *Harvard Review of Psychiatry* 31, no. 3: 162–171. https://doi.org/10.1097/HRP.0000000000000367.

Widge, A. S., K. K. Ellard, A. C. Paulk, et al. 2017. "Treating Refractory Mental Illness With Closed-Loop Brain Stimulation: Progress Towards a Patient-Specific Transdiagnostic Approach." *Experimental Neurology* 287: 461–472. https://doi.org/10.1016/j.expneurol.2016.07.021.

Witt, K., O. Granert, C. Daniels, et al. 2013. "Relation of Lead Trajectory and Electrode Position to Neuropsychological Outcomes of Subthalamic Neurostimulation in Parkinson's Disease: Results From a Randomized Trial." *Brain* 136: 2109–2119. https://doi.org/10.1093/brain/awt151.

Xiao, Y., J. C. Lau, T. Anderson, et al. 2019. "An Accurate Registration of the BigBrain Dataset With the MNI PD25 and ICBM152 Atlases." *Scientific Data* 6, no. 1: 210. https://doi.org/10.1038/s41597-019-0217-0.

Yeh, F.-C. 2022. "Population-Based Tract-To-Region Connectome of the Human Brain and Its Hierarchical Topology." *Nature Communications* 13, no. 1: 4933. https://doi.org/10.1038/s41467-022-32595-4.

Yeh, F.-C., T. D. Verstynen, Y. Wang, J. C. Fernández-Miranda, and W.-Y. I. Tseng. 2013. "Deterministic Diffusion Fiber Tracking Improved by Quantitative Anisotropy." *PLoS One* 8, no. 11: e80713. https://doi.org/10.1371/journal.pone.0080713.

Supporting Information

Additional supporting information can be found online in the Supporting Information section.